

## Physical properties of porous $\text{In}_{0.08}\text{Ga}_{0.92}\text{N}$

Saleh H. Abud<sup>\*</sup>, Z. Hassan<sup>†</sup>, F. K. Yam<sup>‡</sup>

*Nano-Optoelectronics Research and Technology (N.O.R) Laboratory, School of Physics,  
Universiti Sains Malaysia, 11800 Penang, Malaysia.*

### Abstract

In this study, nanoporous structures on  $\text{In}_{0.08}\text{Ga}_{0.92}\text{N}/\text{AlN}/\text{Si}$  thin films with a thickness of  $1\ \mu\text{m}$  were synthesized by photoelectrochemical etching technique at various etching durations. The structural and optical properties of the pre- and post-etched thin films were investigated. The field emission scanning electron microscope images and X-Ray diffraction measurements revealed that the films pre-etched thin film has a sufficiently smooth surface over a large region with wurtzite structure. The roughness increased with an increase in etching duration. The photoluminescence emission peaks had a blue shift phenomenon for the post-etched films at room temperature, compared with the pre-etched film. The photoluminescence intensities of porous InGaN structures were enhanced when the nanoporous structure was formed.

**Keywords:** Porous InGaN; III-nitride; HR-XRD; Photoluminescence.

### 1. Introduction

The wurtzite InGaN layers receive a great deal of attention among III-nitride compound semiconductors because of their direct band gap tuning from 0.7 eV for InN to 3.4 eV for GaN, giving InGaN great potential for the design of high-efficiency optoelectronic devices that operate in the IR, visible, and UV regions of the electromagnetic spectrum [1]. Porous III-nitride compounds are considered as promising materials for optoelectronics [2] and biochemical sensors [3] because of their unique optical and electronic properties compared with bulk materials [4,5]. The formation of a porous nanostructure has been widely reported for crystalline silicon [6]. In addition to porous silicon research, attention has also been focused on other porous semiconductors, such as GaAs [7] and GaN [8]. Interest in porous semiconductor materials arises from the fact that these materials can act as sinks for threading dislocation and are able to accommodate strain. Porous semiconductor materials are also useful for understanding the fundamental properties of nanoscale structures for the development of nanotechnology. Research on porous GaN is strongly driven by the robustness of porous GaN, including its excellent thermal, mechanical, and chemical stabilities that make it highly desirable for optical applications [5]. Many researchers [9-11] have used the photoelectrochemical etching (PEC) technique to synthesize porous GaN, whereas Saleh et al. [1] used this technique to synthesize porous InGaN for the first time. The PEC technique is more suitable and cheaper

<sup>\*</sup>) For correspondence, E-mail: salehhasan71@gmail.com

<sup>†</sup>) For correspondence, E-mail: zai@usm.my

<sup>‡</sup>) For correspondence, E-mail: yamfk@yahoo.com

compared with other techniques for producing high-density nanostructures with controlled pore size and shape [12]. Electrolyte, current density and illumination are the main factors that affect electrochemical etching. Hydrofluoric acid (HF) is the most commonly used material in etching GaAs and GaN.

## 2. Experimental Procedure

### 2.1 Synthesize of Porous $\text{In}_{0.08}\text{Ga}_{0.92}\text{N}$

Porous  $\text{In}_{0.08}\text{Ga}_{0.92}\text{N}$  was prepared using the UV assisted electrochemical etching technique. The etching cell was made from Teflon with platinum wire as cathode and  $\text{InGaN}$  thin film as anode. The native oxide of the samples was initially removed using  $\text{NH}_4\text{OH}:\text{H}_2\text{O}$  (1:20), followed by  $\text{HF}:\text{H}_2\text{O}$  (1:50). Boiling aqua regia  $\text{HCl}:\text{HNO}_3$  (3:1) was subsequently used to clean the samples. The samples were then etched in a solution of  $\text{HF}(49\%):\text{C}_2\text{H}_5\text{OH}(99.99\%)$  with a ratio of 1:5 under UV lamp illumination at different etching durations of 5, 10, and 15 min. All samples were rinsed with ethanol after the etching process and were then dried using nitrogen gas.

### 2.2 Characterizations

The surface morphology and structural properties of the pre- and post-etched  $\text{In}_{0.08}\text{Ga}_{0.92}\text{N}$  thin films were performed using Field emission scanning electron microscope (FESEM, Model FEI Nova NanoSEM 450), atomic force microscope (AFM, Model Dimension EDGE, BRUKER) and high-resolution X-ray diffractometer system (XRD, Model PANalytical X'Pert PRO MRD PW3040, whereas the optical properties were investigated using photoluminescence spectroscopy system (PL, Model Jobin Yvon HR 800 UV), and excited by a He-Cd laser at 325 nm.

## 3. Results and Discussion

Fig. 1(a–d) shows the FESEM images of the pre- and post-etched  $\text{In}_{0.08}\text{Ga}_{0.92}\text{N}$  thin films. In Fig. 1a, the image shows that the grown film has sufficiently smooth surface and uniformly over a large region. Inset is the cross section of the film, the thickness of the  $\text{In}_{0.08}\text{Ga}_{0.92}\text{N}$  and AlN buffer layer is 1  $\mu\text{m}$  and 0.1  $\mu\text{m}$  respectively. Fig. 1(b–d) shows FESEM images of the porous  $\text{In}_{0.08}\text{Ga}_{0.92}\text{N}$  surfaces. Coral-like ridges started to form and the surface became rough during the etching duration of 5 min (Fig. 1b); irregular shapes of ridges with different sizes were found. Increasing the duration to 10 min (Fig. 1c) and 15 min (Fig. 1d) led to increase in the number of forming corals-like ridges, which were the greatest at 15 min. Thus the etching duration affects the shape and size of the formed pores.

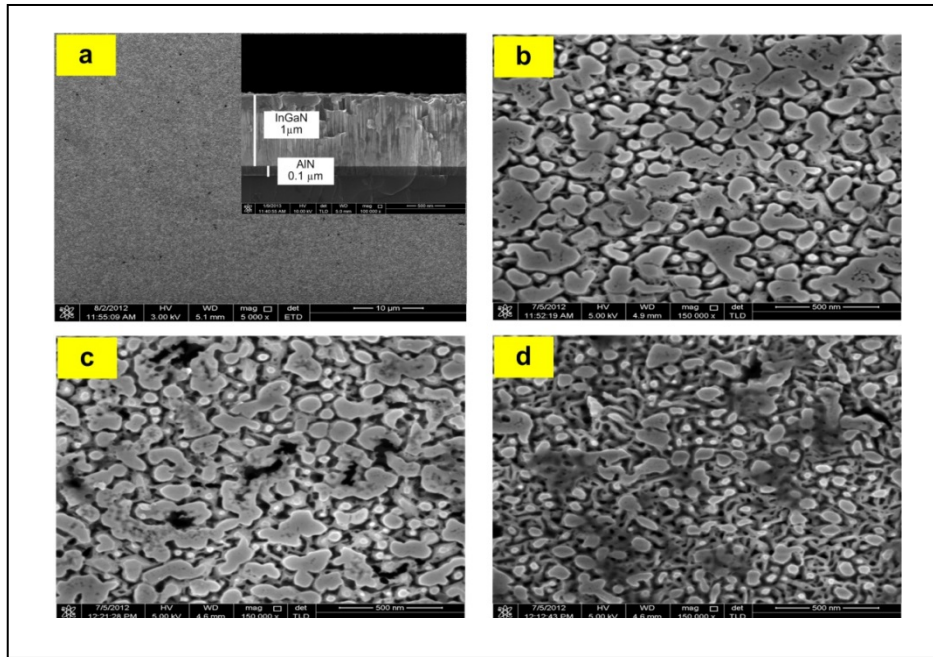


Fig. 1: FESEM image of the as-grown and porous InGaN at various etching durations (a) as-grown, (b) 5 min, (c) 10 min, (d) 15 min.

Fig. 2a depicts  $(5 \times 5) \mu\text{m}$  –AFM image of the grown thin film with a root mean square (RMS) roughness of 2.2 nm. Whereas Fig. 2(b–d) shows the effect of the etching durations on the surface morphology of the etched films. The RMS roughness of the porous films increased with an increase in etching duration to be 27, 193 and 220 nm at 5, 10 and 15 min, respectively. This finding indicates that the roughness of the surface increased with increasing etching durations.

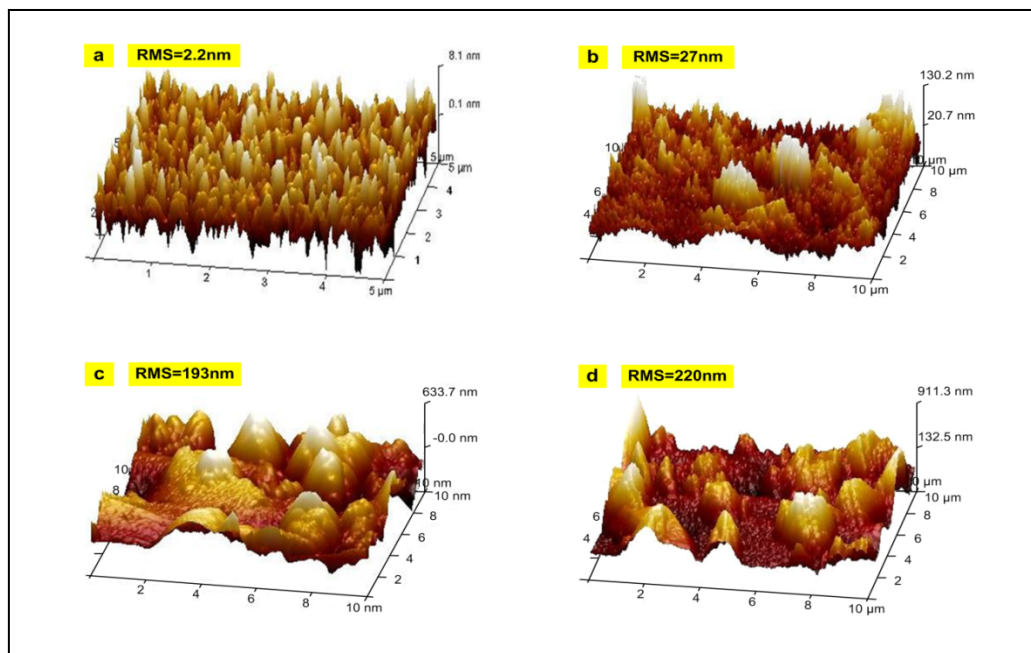


Fig. 2: AFM (3-D) view of of the pre- and post-etched InGaN at various etching durations (a) as-grown, (b) 5 min, (c) 10 min, (d) 15 min.

Fig. 3 shows the X-ray diffraction patterns of the pre- and post-etched InGaN thin films at various etching durations. The diffraction peaks were located at  $34.24^\circ$ ,  $34.28^\circ$ ,  $34.33^\circ$ , and  $34.36^\circ$  relative to the (0002) InGaN pre- and post-etched at 5, 10, and 15 min, respectively. Compared with that of the pre-etched sample, the diffraction peaks of the post-etched samples shifted to a higher-angle region (approaching the GaN diffraction peak), indicating that the indium fraction gradually decreased progressively as etching duration increased. The peak located at  $36.17^\circ$  relative to the (0002) AlN buffer layer. No diffraction peak was observed for InN, which indicate that phase segregation did not occur [13, 14]. With the increase in value along with longer duration, the intensity of the porous thin films reached maximum value at 15 min.

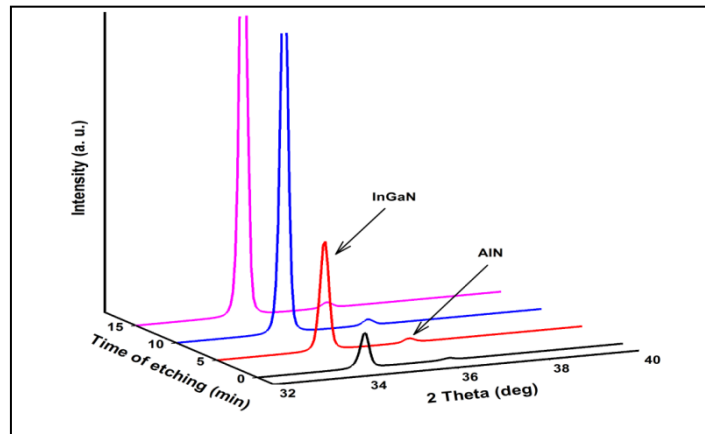


Fig. 3: XRD of the pre- and post-etched InGaN formed at different etching durations.

Fig. 4 shows the photoluminescence (PL) spectra of the thin films at pre- and post-etching for 5, 10, and 15 min. The PL wavelength emission peak at 403 nm is related to the as-grown film. Slight blue shifts were observed in the porous films at wavelengths of 399, 395, and 392 nm which correspond to the etched films at 5 min, 10 min, and 15 min, respectively. These shifts observed in the porous films can be attributed to the change in etching time, which results in quantum confinement effects of particles [15]. The PL intensity of the etched films increased with increasing etching time, and reached the maximum value at 15 min.

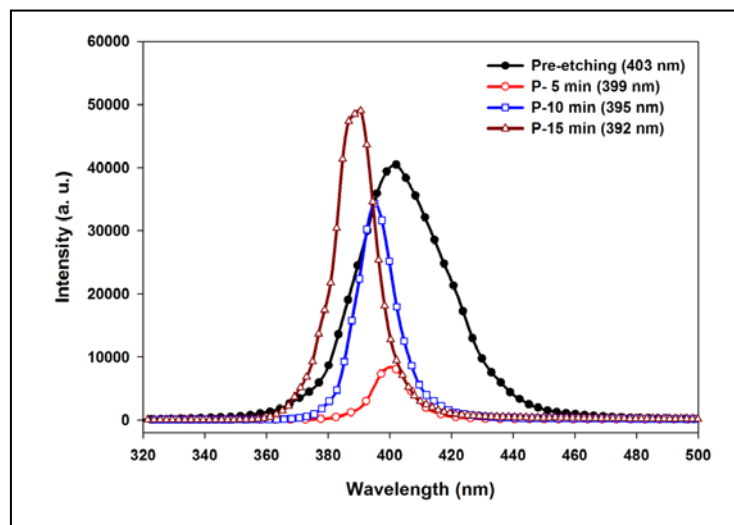


Fig. 4: PL spectra of the as-grown and porous InGaN formed at different etching durations.

#### 4. Conclusion

In summary, we demonstrated an  $\text{In}_{0.08}\text{Ga}_{0.92}\text{N}/\text{AlN}/\text{Si}(111)$  thin film with a thickness of  $1\ \mu\text{m}$  and has a single (0002) peak in its XRD pattern. The thin film has a good quality with wurtzite structure. The porous nanostructures of the films were synthesized using the UV-assisted electrochemical etching method at etching time of 5, 10, and 15 min. Blue shift in PL spectra changed the energy band gap of the sample. This study pointed out that the nanostructures can open a new and promising area in ternary III-nitride materials by choosing suitable etching factors to enhance the structural and optical properties of thin films for optoelectronic devices.

#### Acknowledgments

The authors gratefully acknowledge support from Research University (RU) Grant and Universiti Sains Malaysia.

#### References

- [1] S. H. Abud, Z. Hassan, F. K. Yam, Enhancement of Structural and Optical Properties of Porous  $\text{In}_{0.27}\text{Ga}_{0.73}\text{N}$  Thin Film Synthesized Using Electrochemical Etching Technique. *Int. J. Electrochem. Sci.* **7** (2012) 10038-10046
- [2] A. W. Burton, K. Ong, T. Rea, I. Y. Chan, On the estimation of average crystallite size of zeolites from the Scherrer equation: A critical evaluation of its application to zeolites with one-dimensional pore systems, *Microporous and Mesoporous Mater.* **117** (2009) 75-90
- [3] L. T. Canham, Silicon quantum wire array fabrication by electrochemical and chemical dissolution of wafers, *Appl. Phys. Lett.* **57** (1990) 1046-1048
- [4] Z. Hassan, Y. Lee, F. Yam, K. Ibrahim, M. Kordesch, W. Halverson, P. Colter, Characteristics of low-temperature-grown GaN films on Si (111), *Solid State Commun.* **133** (2005) 283-287
- [5] G. Korotcenkov, B. Cho, Porous semiconductors: Advanced material for gas sensor applications, *Crit. Rev. Solid State Mater. Sci.* **35** (2010) 1-37
- [6] C. F. Lin, Z. J. Yang, J. H. Zheng, J. J. Dai, High-efficiency InGaN light-emitting diodes via sidewall selective etching and oxidation, *J. Electrochem. Soc.* **153** (2006) G39-G43
- [7] A. Loni, L. Canham, M. Berger, R. Arens-Fischer, H. Munder, H. Luth, T. Benson, Porous silicon multilayer optical waveguides, *Thin Solid Films.* **276** (1996) 143-146
- [8] E. Moyen, W. Wulfhekel, W. Lee, A. Leycuras, K. Nielsch, U. Gösele, M. Hanbücken, Etching nano-holes in silicon carbide using catalytic platinum nanoparticles. *Appl. Phys. A* **84** (2006) 369-371
- [9] M. Nahidi, K. W. Kolasinski, Effects of stain etchant composition on the photoluminescence and morphology of porous silicon, *J. Electrochem. Soc.* **153** (2006) C19-C26
- [10] A. Ramzy, Z. Hassan, K. Omar, Porous GaN on Si(111) and its application to hydrogen gas sensor, *Sens. Actuators, B* **155** (2011) 699-708.
- [11] C. B. Soh, S. Y. Chow, L. Y. Tan, H. Hartono, W. Liu, S. J. Chua, Enhanced luminescence efficiency due to carrier localization in InGaN/GaN heterostructures grown on nanoporous GaN templates, *Appl. Phys. Lett.* **93** (2008) 173107

- [12] C. B. Soh, W. Liu, H. Hartono, N. S. Ang, S. J. Chua, A. P. Vajpeyi, Enhanced optical performance of amber emitting quantum dots incorporated InGaN/GaN light-emitting diodes with growth on UV-enhanced electrochemically etched nanoporous GaN. *Appl. Phys. Lett.* **98** (2011) 191906-191903
- [13] S. H. Abud, Z. Hassan, F. K. Yam, A. J. Ghazai, Structural and Optical Properties of  $\text{In}_{0.27}\text{Ga}_{0.73}\text{N}/\text{Si}$  (111) Film Grown Using PA-MBE Technique. *Adv. Mater. Res.* **620** (2013) 368-372.
- [14] S. H. Abud, A. Ramiy, A. S. Hussein, Z. Hassan, F. K. Yam, Superlattices Microstruct, **60** (2013) 224-230
- [15] F. K. Yam, Z. Hassan, A. Y. Hudeish, The study of Pt Schottky contact on porous GaN for hydrogen sensing, *Thin Solid Films.* **515** (2007) 7337-7341